

## **EVALUATION OF THE PREDICTIVE SEGMENTATION ALGORITHM FOR THE LASER TRIANGULATION METHOD**

**Jacek Reiner, Maciej Stankiewicz**

Wrocław University of Technology, Institute of Machine Technology and Automation, Wybrzeże Wyspiańskiego 27, 50-370 Wrocław, Poland  
(✉ jacek.reiner@pwr.wroc.pl; maciej.stankiewicz@pwr.wroc.pl)

### **Abstract**

Laser triangulation is one of the machine vision measurement methods most commonly used in 3D quality control. However, considering its susceptibility to interference, it cannot be used in certain areas of industrial production e.g. very shiny surfaces. Thus, for the improvement of its applicability, a predictive algorithm of light profile segmentation was designed, where – as a result of using *a priori* knowledge – the method becomes resistant to secondary reflexes.

The developed technique has been tested on selected parts with surfaces typical for the machine-building industry. The evaluation has been presented based on the surface representation (mapping) error analysis, using the difference between the obtained cloud of points and the nominal surface as processing data, as well as scatter of the discrete Gauss curvature.

Keywords: laser triangulation, predictive segmentation, discrete Gaussian curvature.

© 2011 Polish Academy of Sciences. All rights reserved

## **1. Introduction**

Commonness of the *zero defects* strategy in numerous industry branches – among others in medicine, aviation, automotive – sets huge challenges to applications related to manufacturing technology as well as quality assurance and metrology. One hundred percent quality control of production in the German automotive industry is used in more than 23% of production plants of this industry. In relation to that, within the last several years, a rapid development in the fast measurement methods has been observed. In the same group of enterprises, only 15,5% have not implemented the 3D measurement systems yet. The highest percentage of such equipment (44,6%) has been used in the quality control departments. Among them, as much as 36.2% of solutions is based on the laser triangulation method [1].

### **1.1. Laser triangulation technique**

One of the most commonly used 3D inspections in the in-process quality assurance systems is the laser triangulation method [2, 3]. Its main advantages are contactless use, possibility of full automation and it is faster than point scanning methods, eg. conoscopy, confocal microscopy. It may also operate in the environment of disturbance coming from such powerful sources as arc welding [4]. Numerous industrial implementations are already available, which successfully expand the field of their application. Most frequently, these are complete 3D scanners having at their disposals the powerful software and measurement resolution of several micrometers [1]. It enables building of an advanced automatic measurement and/or inspection system at a relatively low cost.

Unfortunately, the solution has also certain limitations, which are particularly apparent in the machine building industry. The dominant product there are metal parts with high quality

machined functional surfaces, destined for co-operation with other ones. They are characterized by low roughness, sometimes manifesting itself with high surface gloss (shine). Light reflected from them, including laser light, causes reflexes which disturb – and sometimes even disable – the measurement. Classical segmentation algorithms are not able to distinguish them from the main line of the light profile the scanned part height is to be determined from. Among the more advanced, as the most universal method is considered the method of narrowing the search area beam [5, 6], but also its performance limitations and the requirement for additional equipment and multiple acquisitions are indicated.

The laser triangulation method is used for different scales, starting from micro where surface topography is measured. This work concentrates solely on macro applications, where the geometry of machine elements is scanned. In this paper we focus on the automatic dimensional inspection of products.

### ***1.2. The developed solution***

A segmentation algorithm immune to the secondary light reflexes has been developed [7]. Its operation consists in prediction of the light line position based on the nominal CAD 3D model of the scanned object, which is in a dynamic way parametrizing the segmentation module. Due to predicting the system state, it is also possible to increase the triangulation measurement accuracy – particularly in case of scanning free form surfaces and parts with variable parameters, such as color or roughness. A limitation of the elaborated method is the necessity of knowledge of the scanned object model.

As parts of the whole system, also the synchronising method and the laser triangulation control system have been developed. A test setup was built and the whole was verified using exemplary parts typical for the machine building industry. The article presents the operation principle of the created solution along with the bibliographical references describing individual work stages. The verification process of the elaborated method, along with its results, has been presented in more details.

## **2. Predictive segmentation**

In order to widen applicability of the laser triangulation method (LTM) also to scanning the shiny surfaces of complex shapes, an algorithm has been developed, which uses CAD model of the scanned part for predictive narrowing down the area of laser line search.

The algorithm is forming an expansion of the classic process of 3D representation in the LTM, which has been presented in Fig. 1. The classical algorithm of the triangulation image segmentation calculates positions of the laser line in each image column, and then converts them to points in the 3D space. As shown in the diagram in Fig. 1, it is preceded here with a prediction stage, the task of which is dynamic determination of the confidence interval, where the laser profile will be searched for. Such interval is the area at the triangulation image where the probability of the main laser line appearance is the highest.

Subsequent steps of the prediction are, as shown, identical to the steps of the process of point extraction from an image and their 3D conversion in the course of usual LTM calculations. What is obvious, they run in reverse sequence.

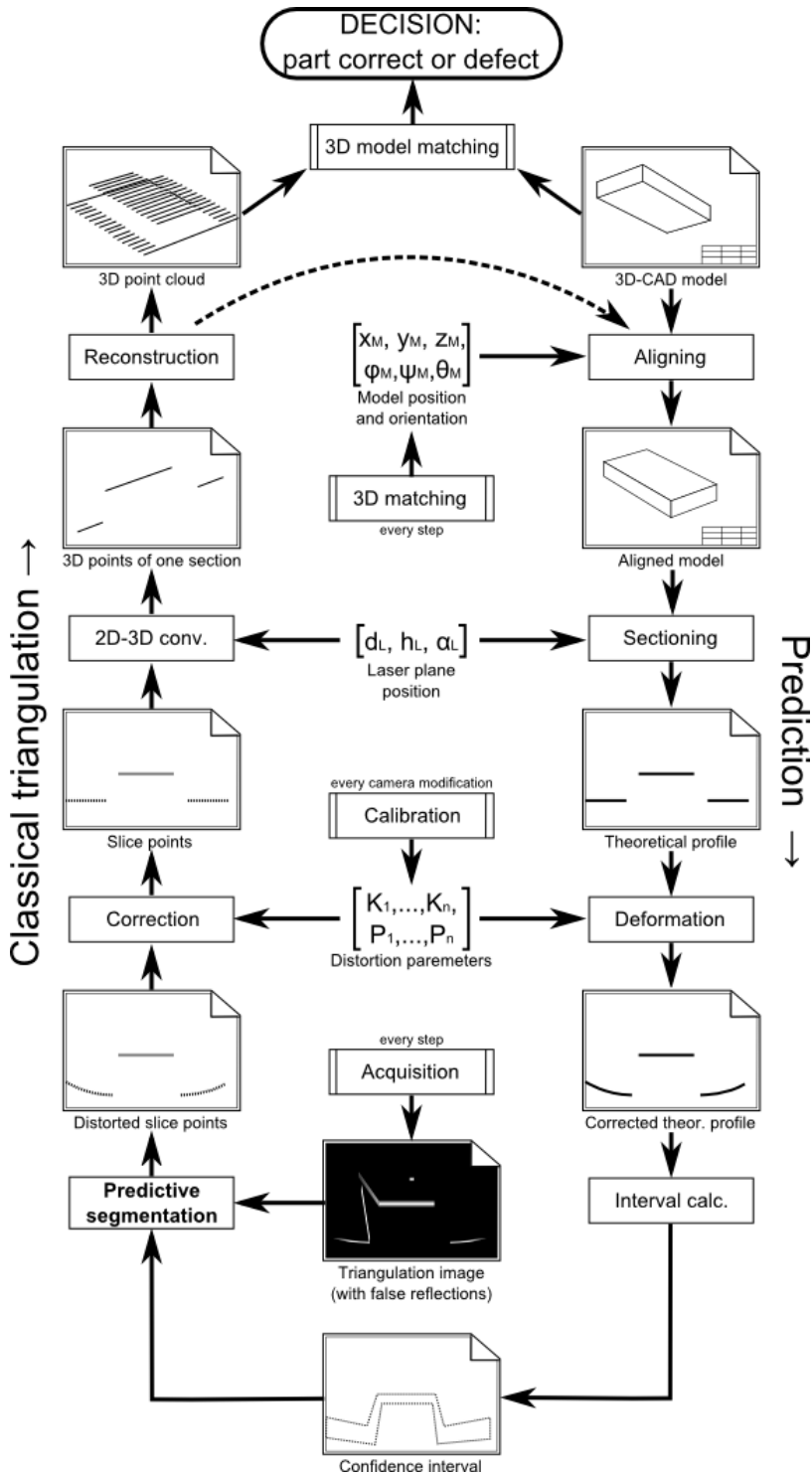


Fig. 1. Schematic diagram of the predictive segmentation algorithm with the CAD3D model.

## **2.1. Model synchronization**

The 3D-CAD model of the scanned object is being synchronized (aligned) according to the real part position and orientation. Predictive segmentation algorithm requires reliable way of aligning the model with reality. This means readjustment of the CAD model inside the virtual laser triangulation system. Position and orientation of the virtual scanned part must be compatible with reality and the synchronization is repeated every scanning step. In the opposite case the theoretical and real laser line will not be coherent, causing improper operation of the whole algorithm. Synchronization accuracy strongly influences the ability of the algorithm to predict and, consequently, the measurement accuracy. Even small changes in the scanned part geometry may cause high changes in the image. This is particularly valid in the vicinity of discontinuities and sharp changes in the object geometry (e.g. edges and holes). In the developed solution an additional positioning camera was applied. Its vision field involves the whole space of the test stand. Such solution enables scanning at high rates [8].

## **2.2. Shape and light profile position modeling**

Operation of the predictive segmentation algorithm is based on extracting information on the predicted position of the laser line from the especially developed CAD environment. In that environment both, the triangulation system – a camera and a laser line projector, as well as the nominal model of the scanned part are modeled. Based on the data, a theoretical image of the light profile is generated, the one that should be obtained at the triangular camera sensor. It creates a base for determining the area in which – with the highest probability – the laser line will appear in the real image.

For easier configuration of the virtual triangulation setup, the graphic interface was also programmed.

Operation of the above described module has been described in detail in [7].

## **2.3. Profile deformation**

Synthetic images of the theoretical light profile, obtained from the CAD 3D model (see section 2.2. *Shape and light profile position modeling*), are „ideal” – i.e. created on the basis of the nominal part model, according to the simplified camera model in the form of a simple perspective projection [9, 10]. Images obtained from the cameras, not having at their disposal the special optics, are meanwhile deformed to a certain degree by optical phenomena called, in general, distortion. Thus, the effect significantly influences the coherence between the theoretical laser profile determined in the predictive way and its real image obtained from a camera [11].

For that reason after every camera modification, e.g. changing the lens, focusing, aperture adjustment (see Fig. 1) it is necessary to recalibrate the acquisition setup.

During work on the predictive segmentation algorithm, the available distortion reduction methods were thoroughly analyzed and the optimal solution for the formulated application has been elaborated. The complete set of procedures for calibration of the triangular system for the presented algorithm needs has been programmed. The work has been described in more detail in [12].

## 2.4. Determination of the confidence interval

Prediction of the laser line position in an image is implemented in the form of the Kalman filter set [13, 14], where each loop determines the position of profile centre in one column of the triangulation image.

All classic laser line segmentation algorithms assume a symmetric distribution of light intensity across the laser line. The assumption is fulfilled in case of measurements of uniform, ideally dissipating planes. If the tested surface is not a plane, or its parameters are variable, then the asymmetry of distribution is evident. Meanwhile, it causes irregular measurements of the light profile centre with classical methods [15].

## 3. Evaluation of the developed method

Evaluation is based on tests performed on real parts selected so as to represent typical parts for the machine building industry, including the features introducing obstacles for laser triangular method application (e.g. glossiness, complex shape).

For verifying the algorithm operation on a free-form surface, it was decided that, besides the classic analysis of absolute errors, the parameter called the discrete Gaussian curvature [16] was also calculated.

To each point from the obtained scanning point cloud ( $P_0$ ) an additional parameter  $K$  was assigned. It is called discrete Gaussian curvature and defined in equations (1) and (2). It is proportional to the sum of all triangular angles  $\Theta_i$  the vertex of which is the considered point  $P_0$  (Fig. 2), and describes the localization of a given point in relation to its closest neighborhood. Variables used in (1) and (2) are shown in Fig. 2. The operator in the numerator in (2) is the vector dot product. Vectors  $v_i$  are defined as  $v_i = P_i - P_0$ . The value must be within the range of  $0 \div 2\pi$ . The angle 0 means that the point would have to lie in infinity, or all the vertexes considered are identical. The maximum angle would indicate that the considered point  $P_0$  lies in one plane with all the points from its direct vicinity ( $P_i$ ). Recapitulating, a high value of parameter  $K$  indicates that the point is very distant from the remaining ones (*outsider*), while high scatter of the  $K_i$  values for all surface points (high standard deviation  $-s_K$ ) means that it is not smooth but uneven.

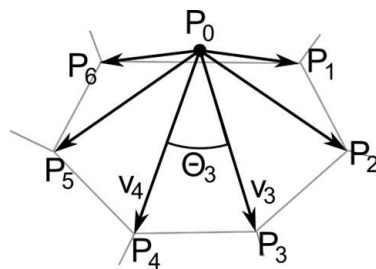


Fig. 2. Graphical representation of curvature  $K$  evaluation [15].

$$K = 2\pi - \sum_i \theta_i, \quad (1)$$

$$\theta_i = \arccos \left( \frac{\vec{v}_i \bullet \vec{v}_{i+1}}{|\vec{v}_i| |\vec{v}_{i+1}|} \right). \quad (2)$$

Thanks to comparison of the  $s_K$  scatters for different scanning methods the information is to be obtained, which one of them is correctly reflecting the type of surface (even/uneven).

Using that method, the results from scanning one part, performed with different measurement tools could be compared and determined which one of them is better reflecting the character of the nominal part [17].

### 3.1. Test stand

In order to verify the developed predictive segmentation method, a configurable 3D laser triangulation stand was elaborated and set up (Fig. 3), enabling flexible change of position and orientation of its optical components and detectors within the tested range. It consists of a monochromatic digital matrix camera with appropriate lens, a focusable laser line generator, a a computer-controlled precise X-Y stage and a PC with image acquisition, motion control and data analysis software.

Due to the application of positioning scales and precise drives with encoders, it was possible to modify the stand settings without the necessity of its recalibration.

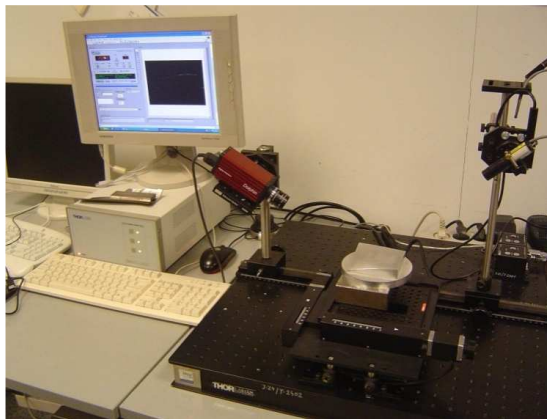


Fig. 3. Test stand for verification of the predictive segmentation algorithm in the LTM.

### 3.2. Software for method testing

Because of the prototype character of the verifying setup, the software was divided into an acquisition part responsible for image collection, and a calculation part being the actual implementation of the predictive segmentation algorithms, as well as others necessary for the laser triangulation method.

The program operates offline using data recorded on the computer disk. For the automatic acquisition of triangulation images, as well as for their initial processing, an interface controlling the drives and cameras operation was created with the use of rapid application development environment.

### 3.3. The tested parts

For the purpose of method verification the test specimens presented in Fig. 4 were used. For the exact quantitative verification of the reflex effect a steel vee block and an aluminum part of especially prepared free glossy surface were used. Both of them are chosen so that they

have geometrical, surface and material properties emphasizing the typical problems arising during laser scanning of industrial parts.

For knowledge of their geometry, all of them were measured tactile (CMM) and with use of fringe pattern method in the accredited Laboratory of Reverse Engineering of the Wrocław University of Technology.

During the tests, the above measurements of the prepared parts were performed.

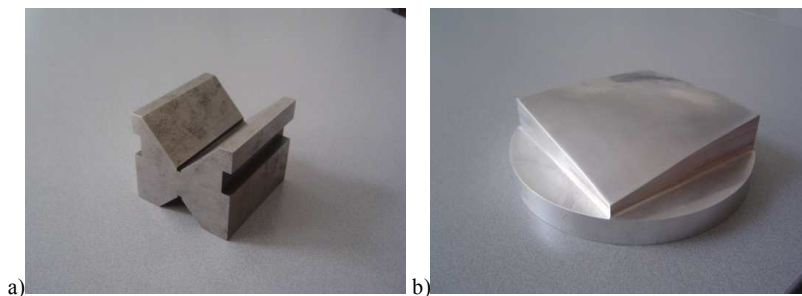


Fig. 4. Test specimens for quantitative and qualitative verification of the predictive algorithm: a – vee block, b –glossy free-form surface.

### 3.4. Qualitative verification results

During tests the prepared parts were scanned with the use of the predictive segmentation algorithm as well as without it. The obtained results were subjected to comparative study, in which the influence of the applied method on the representative error value was determined.

#### Object A – vee block

The scanned vee block surface (4a) is featured by an inclination angle of  $45^\circ$  in relation to the axis of the optical system and a surface roughness of  $R_a=0.4$ .

Results of its scanning have been presented in Figs 5a and 5b. A distinct influence of the reflexes disturbing the classic algorithm and effectiveness of the developed predictive algorithm is visible there.

Fig. 5a shows clearly the influence of disturbances in the form of artifacts caused by internal reflexes of the laser line in the glossy (mirror) surfaces of the block.

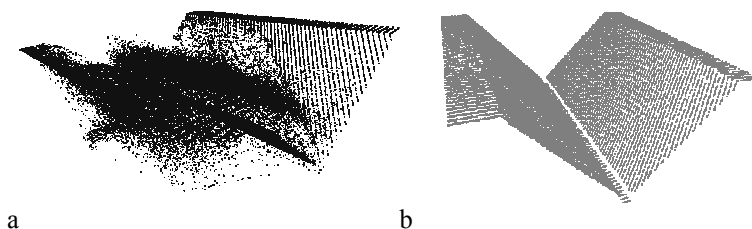


Fig. 5. Vee block scanning result without (a) and with (b) use of the predictive algorithm.

#### Object B – free-form surface

In the image of the cloud of points obtained with the classical method - Fig. 6a, the two groups of substantial disturbances are visible. They do not appear in case of applying the predictive algorithm – Fig. 6b.



Fig. 6. Free form surface scanning result without (a) and with (b) the use of predictive algorithm.

A schematic diagram of reflex formation has been presented in Fig. 7. Despite the source of their origin, they are being eliminated. That type of reflexes is a frequently met disturbance in the laser triangulation method. They result from local setting of surface in such a way that the laser light incidence angle is equal to the camera vision angle. A strong reflex from a smooth surface, directed straight into the objective, causes oversaturation of pixels on the large surface. In the picture it is seen in the form of a spot, which disables a correct operation of the classical algorithms of segmentation.

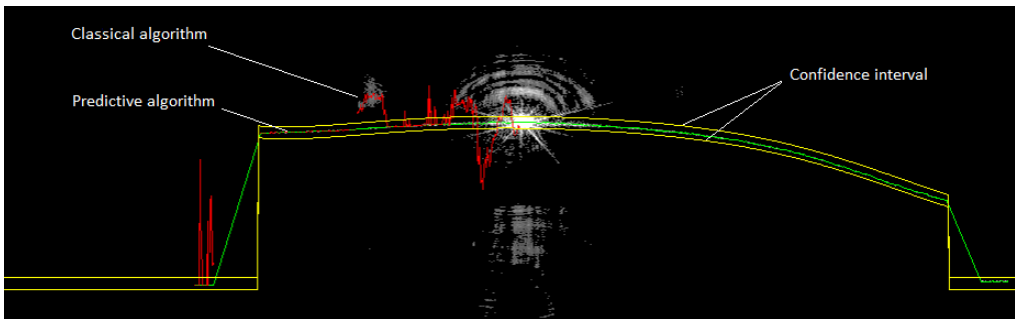


Fig. 7. Triangulation image with specular reflection.

### 3.5. Quantitative verifications results

Measurement results obtained in the tests with the use of classical and predictive algorithms of light profile segmentation were compared with the aim of determining the increase in accuracy of the laser triangulation method. For qualified verification of the developed method the residuals maps (maps of errors) were calculated. The error maps elaboration consists in determining for each point obtained from the cloud the distance from the nearest surface defining the model body.

#### **Object A – vee block**

Fig. 8 presents the ideal model of object from Fig. 4a with superimposition of the over-scaled cloud of points obtained during part scanning using the predictive segmentation algorithm, as well as the qualitative results of the models comparison. In the extreme points the deviations within the  $-0.16$  mm, to  $+0.12$  mm range were found, however the majority of measurements lies in the range  $0 \pm 0.05$ .

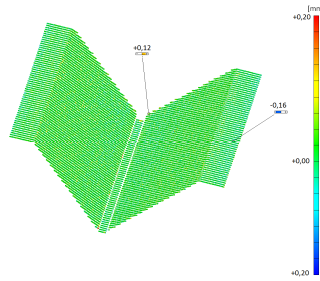


Fig. 8. Qualitative view of surface comparison.

Comparison of the vee block scanning results using the ordinary algorithm was impossible, as the number of artifacts, treated by the software as outliers, was too big to obtain reasonable results – Fig. 9.

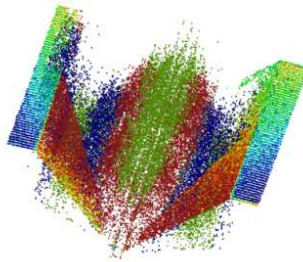


Fig. 9. A trial of comparison of the scanning result with use of the ordinary algorithm of segmentation.

### ***Object B – glossy free-form surface***

The object represents a free-form surface machined manually, with a roughness of  $R_a = 0.2$ .

Fig. 10 presents scanning error maps for point clouds of object B, obtained with the use of the predictive (a) and ordinary (b) segmentation algorithms. Measurement results for surface fragments free from interference do not differ in principle from each other. However, operation of the new algorithm for minimizing the effects of reflections is important for significant diminishing the errors as a whole.

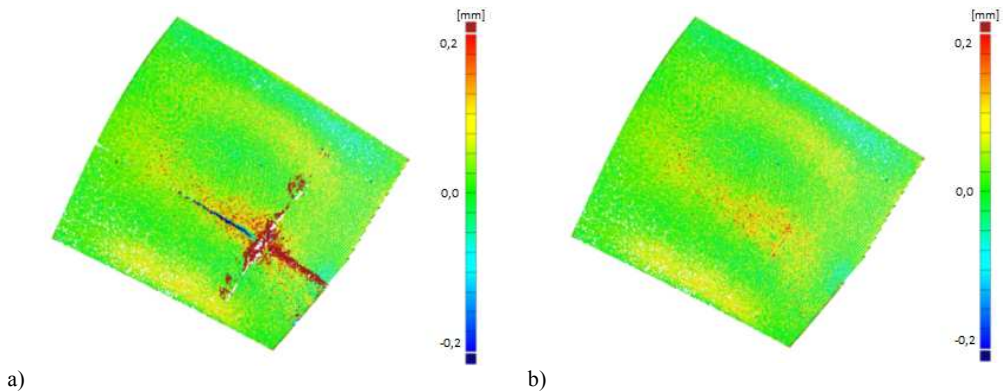


Fig. 10. Error maps (thr. 60) for scanning with the use of classical (a) and predictive (b) algorithm.

Tests at specimen B confirm that scattered values of error for the measured values are much lower in case of applying the predictive segmentation algorithm, which is evidenced by histograms in Fig. 11 and data collected in Table 1.

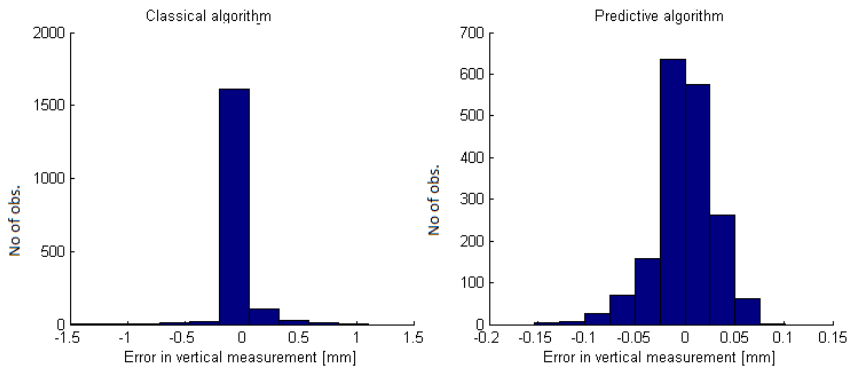


Fig. 11. Residuals histograms for classical (left) and predictive (right) algorithms.

The effect of narrower error scatter in case of diminishing the threshold in the predictive algorithm results from more effective prediction of the laser line position in case of its decay at an image. It has been achieved due to the use of the Kalman filter. For a change, the classical algorithm, in case of profile decay in the vision field, returns the *not-a-number* value visible at surface images as a discontinuity.

Table 1. Standard deviation of the profile localization residuals for two algorithms.

Threshold	60	80	100	120
Classical segmentation	32.44	37.82	46.29	56.23
Predictive segmentation	1.41	1.38	1.31	1.22

Surface analysis with use of the discrete Gauss curvature also confirms that the predictive segmentation algorithm enables significantly better surface reconstruction. It has been shown in Fig. 12 and 13.

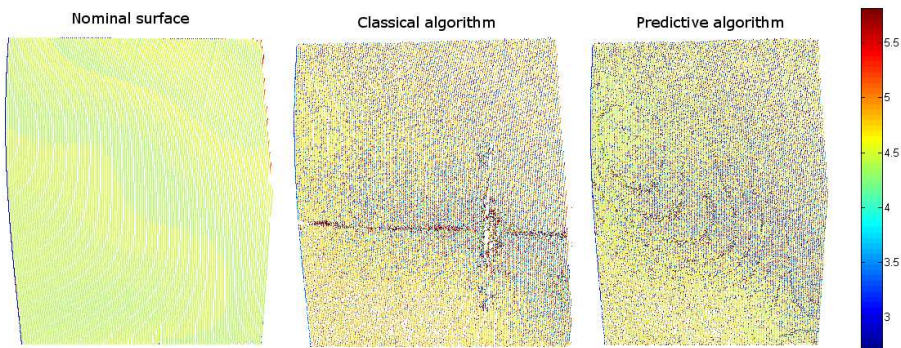


Fig. 12. Values of the discrete Gauss curvature at the discussed surfaces.

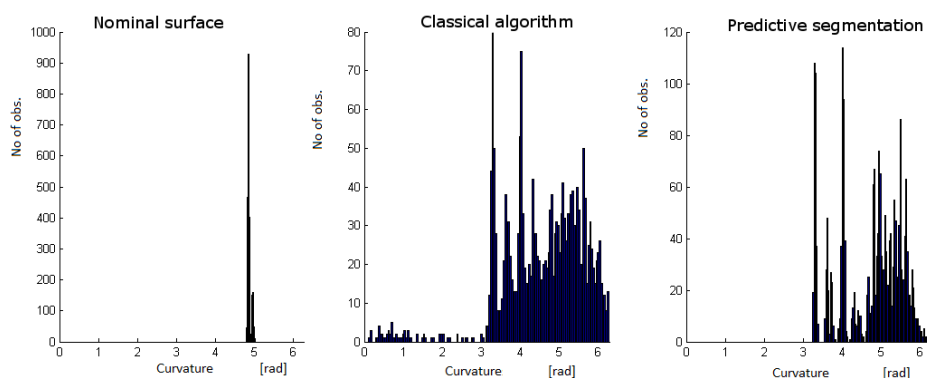


Fig. 13. Distributions of the discrete Gauss curvatures in the surrounding of the main interference.

Curvatures of the nominal surface are contained within the 4.2÷4.8 rad interval. Both scanned surfaces have greater curvature range, which is caused by the representation errors. Scanning with the use of the predictive algorithm causes a decrease in the discrete Gauss curvature value spread.

#### 4. Conclusions

For reduction of light reflexes, disturbing the profile segmentation in the triangulation method, a positioning and synchronization algorithm was developed, as well as the theoretical light profile position in the CAD 3D model. The algorithm, for the known and set configuration of the measurement stand and the surface parameters, determines the confidence interval of the light profile positioning for the segmentation module, which is narrowing the search field and increases the resistance of its operation.

Tests were performed, aimed at determining the robustness of the new algorithm, in case of the measurement of strongly reflexive surfaces. The developed solution was tested on the example of selected parts with surfaces typical for the machine building industry. Verification was presented on the basis of residuals analysis in surface representation, using as the data the differences between the obtained point cloud and the nominal surface, as well as using the scatter in the discrete Gaussian curvature.

The research conducted has confirmed that the developed predictive segmentation algorithm significantly increases the glossy surface representation accuracy. Simultaneously, high sensitivity of the method to errors resulting from inaccuracy in geometric calibration and non-repeatability of the manipulation system were observed.

#### Acknowledgements

The scientific work was financed from the means assigned to Science within 2007-2010, as the research project No. N N503 2319 33.3.

#### References

- [1] Sackewitz, M. (2010). 3D-Messtechnik in der deutschen Automobil- und Zulieferindustrie. Fraunhofer Allianz Vision.
- [2] Zhou, F., Zhang, G. (2005). Complete calibration of a structured light stripe vision sensor through planar target of unknown orientations. *Image and Vision Computing*, (23), 59-67.

- [3] Dorsch, R.G., Häusler, G., Herrmann, J.M. (1994). Laser triangulation: fundamental uncertainty in distance measurement. *Appl. Opt.* (33), 1306-1314.
- [4] Tzafestas, S.G. (1999). *Advances in Intelligent Autonomous Systems*. Kluwer, Dordrecht/Boston.
- [5] Jihong, Chen, Daoshan, Yang, Huicheng, Zhou, Shaw Buckley. (1998). Avoiding Spurious Reflection From Shiny Surfaces on a 3D Real-Time Machine Vision Inspection System. *IEEE Instrumentation and Measurement, Technology Conference* St. Paul, Minesota, USA.
- [6] Dea-Gyu, Kim, Won-Seok, Chang, Seung-Kyu, Park, Sung-Hoon, Bauk, Cheol-Jung, Kim. (1999). A Study on 3D Profilometer Using Dynamic Shape Reconstruction with Adaptive Pattern Clustering of Line-Shaped Laser Light. *IEEE Tencon*.
- [7] Reiner, J., Stankiewicz, M., Wójcik, M. (2009). Predictive segmentation method for 3D inspection accuracy and robustness improvement. *Optical measurement systems for industrial inspection VI*, Munich, Germany / ed. Peter H. Lehmann. Bellingham, Wash.: SPIE - The International Society for Optical Engineering, 73890A-1 - 73890A-8.
- [8] Stankiewicz, M., Reiner, J., Kotnarowski, G. (2011). Positioning of scanned part inside of the laser triangulation system. *Proceedings of SPIE Optical Metrology Conference*, 8082, Munich.
- [9] Weng, J., Cohen, P., Herniou, M. (1992). Camera Calibration with Distortion Models and Accuracy Evaluation. *IEEE Transactions on Pattern Analysis and Machine Intelligence*, 14(10), 965-980.
- [10] Eisert, P. (2002). Model-based Camera Calibration Using Analysis by Synthesis Techniques. *Publications Heinrich-Hertz-Institute*, Erlangen, Germany.
- [11] Heikkilä, J. (2000). Geometric Camera Calibration Using Circular Control Points. *IEEE Transactions on Pattern Analysis and Machine Intelligence*, 22(10).
- [12] Reiner, J., Stankiewicz, M. (2010). Elimination of distortion of geometric image in method of laser triangulation. *Measurement, Automation, Control*, 56, 1, 54-57. (in Polish)
- [13] Kalman, R.E. (1960). A New Approach to Linear Filtering and Prediction Problems. *Transactions of the ASME Journal of Basic Engineering*, 82, 35-45.
- [14] Simon, D. (2006). *Optimal State Estimation: Kalman, H Infinity, and Nonlinear Approaches*. Wiley
- [15] Hanczak, A. (1991). Fusion of range and intensity data in a scanning sensor, *SPIE vol. 1614 Optics, Illumination, and Image Sensing for Machine Vision VI*.
- [16] Vezzetti, E. (2010). Pitch function comparison methodology for supporting a smart 3D scanner selection. *Precision Engineering*, 34, 327-337.
- [17] Orazi, L., Tani, G. (2007). Geometrical inspection of designed and acquired surfaces. *Int. Journal of Advanced Manufacturing Technology*, 34.